DOI: 10.1002/cphc.201000200

Dioxygen Reduction by Cobalt(II) Octaethylporphyrin at Liquid | Liquid Interfaces

Raheleh Partovi-Nia,[a] Bin Su,[a] Manuel A. Méndez,[a] Benoit Habermeyer,[b] Claude P. Gros,[b] Jean-Michel Barbe,[b] Zdenek Samec,[c] and Hubert H. Girault*[a]

Oxygen reduction catalyzed by cobalt(II) (2,3,7,8,12,13,17,18-octaethylporphyrin) [Co(OEP)] at soft interfaces is studied by voltammetry and biphasic reactions. When Co(OEP) is present in a solution of 1,2-dichloroethane in contact with an aqueous acidic solution, oxygen is reduced if the interface is positively polarized (water phase versus organic phase). This reduction reaction is facilitated when an additional electron donor, here ferrocene, is present in excess in the organic phase.

Introduction

The oxygen reduction reaction (ORR) is a key reaction in life processes, such as respiration, and in energy-converting systems, such as fuel cells, or even for electrochemical sensors design. So far, many catalytic systems are based on the use of expensive noble-metal catalysts, but a lot of effort is dedicated to the development of catalytic systems based on transition-metal complexes.[1] In this context, metalloporphyrins have been widely investigated as promising candidates for catalyzing ORR,[2] and numerous studies have examined the electrocatalytic reduction of dioxygen at metalloporphyrin-modified electrodes. Usually, monomeric metalloporphyrins can reduce oxygen to form hydrogen peroxide through a two-electron pathway, and more complex bimetallic systems that can trap molecular oxygen between the two metal centers, such as Pacman cofacial dyads, are required to promote the direct reduction of oxygen to water via a four-electron pathway. These dyads include biscobalt bisporphyrin,[3] biscobalt porphyrin-corrole, and biscobalt biscorrole derivatives.[4]

The catalytic activity toward the reduction of oxygen has been extensively investigated using the modified electrode methodology (rotating ring disk electrode, RRDE)[5] or using molecular electron donors, such as ferrocene (Fc) and its derivatives in homogeneous solutions[6]. The reduction of O_2 by Fc and its derivatives in acidic solution proceeds rather slowly while the presence of catalytic amounts of an appropriate metalloporphyrin can significantly accelerate the reaction rate.[7] Employing Fc derivatives as electron donors, O_2 reduction catalyzed by cobalt(II) (2,3,7,8,12,13,17,18-octaethylporphyrin) [Co(OEP)] and other cobalt porphyrins has been investigated by Fukuzumi et al. in organic media in the presence of a soluble organic acid.[6]

Another way to study the catalytic properties of different porphyrins is to study oxygen reduction at polarized liquid | liquid interfaces. Indeed, such interfaces can be polarized, that is, the potential difference between the two phases can be controlled; they also offer the possibility to physically separate reactants, such as the protons in water and the electron donors in the organic phase, to carry out interfacial proton-coupled electron-transfer (PCET) reactions.[8] Therefore, the electrochemical control of the interface between two immiscible electrolyte solutions (ITIES) provides a very efficient method to control the rates of either proton or electron transfer across the interface that are both potential-dependent, which is interesting considering that ORR is a PCET reaction. It should be mentioned that in a classical voltammetry using a solid electrode, one measures a current response associated to the electron-transfer step but not to the proton-transfer step.

Herein, proton-coupled oxygen reduction by Fc involving Co(OEP) as a catalyst at a polarized water | 1,2-dichloroethane (1,2-DCE) interface is reported. We show that Co(OEP) serves as a redox catalyst—like conventional cobalt porphyrins—activating O_2 reduction via coordination to the cobalt(II) center by the formation of a superoxide structure.[9] Moreover, we also find that Co(OEP) can reduce oxygen by itself in the absence of any sacrificial electron donor. The present system provides an example of molecular electrocatalysis for oxygen reduction where a molecular catalyst is used like in homogeneous catalysis, but the reaction is electrocatalytic because the ORR depends on the applied Galvani potential difference between the two phases.

[a] Dr. R. Partovi-Nia, Prof. B. Su, M. A. Méndez, Prof. H. H. Girault
Laboratoire d'Electrochimie Physique et Analytique
Ecole Polytechnique Fédérale de Lausanne
Station 6, CH-1015, Lausanne (Switzerland)
Fax: (+41) 21-6933667
E-mail: hubert.girault@epfl.ch

[b] B. Habermeyer, Dr. C. P. Gros, Prof. J.-M. Barbe
Institut de Chimie Moléculaire, Université de Bourgogne
ICMUB (UMR 5260), BP 47870, 21078, Dijon Cedex (France)

[c] Prof. Z. Samec
Department of Electrocatalysis
J. Heyrovsky Institute of Physical Chemistry
Academy of Sciences of the Czech Republic
v.v.i, Dolejskova 3, 182 23 Prague 8 (Czech Republic)

Supporting information for this article is available on the WWW under http://dx.doi.org/10.1002/cphc.201000200.

Results and Discussion

Voltammetry of Co(OEP)

Figure 1 a shows cyclic voltammetric (CV) data corresponding to cell 1 in Scheme 1. In this case, the aqueous background electrolyte is HCl and the organic salt is ammoniumtetrakis-(pentafluorophenyl)borate (BATB). The resulting potential window ranges from −0.2 to 0.35 V. The positive edge of this window is determined by the transfer of H^+ whereas the negative edge is determined by the transfer of Cl^- ions from water to 1,2-DCE since the ions composing the organic supporting electrolyte solution, namely, BA^+ and TB^-, are too lipophilic to be transferred within the potential range aforementioned. In the presence of Co(OEP) in the organic phase, the positive current signal observed at potentials above 0.3 V is assigned to a PCET reaction, in which proton transfer and electron transfer are tightly linked to reduce O_2 to H_2O_2, as shown below.

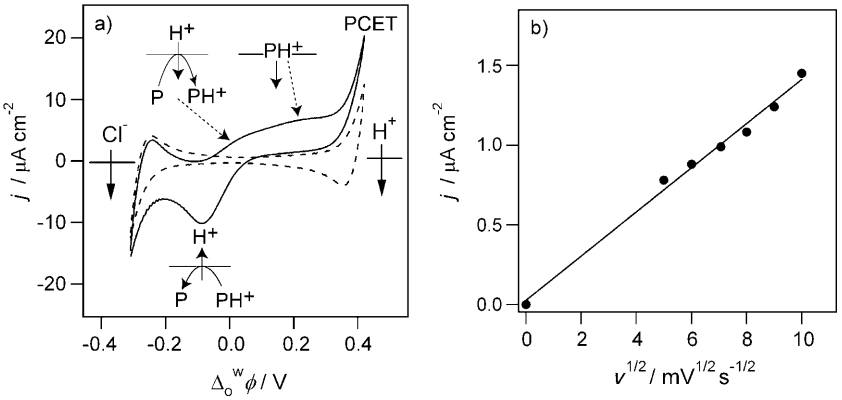

Figure 1. a) Cyclic voltammograms (50 mV s^{-1}) obtained using cell 1 in the absence ($x = 0$, -----) and presence ($x = 200$, ——) of porphyrin P = Co(OEP) in 1,2-DCE; b) The magnitude of the forward current wave at 0 V as a function of the square root of the scan rate.

Cell 1

Ag	AgCl	10 mM LiCl 1 mM BACl	5 mM BATB x μM Co(OEP)	10 mM HCl	AgCl	Ag

Cell 2

Ag	AgCl	10 mM LiCl 1 mM BACl	5 mM BATB x μM Co(OEP) y mM Fc	10 mM LiCl 10 mM HCl	AgCl	Ag

Scheme 1. Electrochemical cells employed.

From the voltammogram in Figure 1 a, measured in the presence of Co(OEP), two waves were observed on the forward scan and only one wave on the reverse scan. The magnitude of the first forward current wave is proportional to the square root of the scan rate (Figure 1 b) and to the concentration of Co(OEP) (see Figure SI-1 of the Supporting Information), indicating a process controlled by the semi-linear diffusion of Co(OEP) to the interface. On the other hand, the current magnitude of the forward waves is independent of the pH of the aqueous phase, but all three waves shown in Figure 2 shift by 60 mV per pH unit towards negative potentials, which indicates that these waves are due to charge-transfer reactions associating both protons and Co(OEP). It can be noticed in Figure 2 that the potential window decreases as the pH decreases, thereby confirming that the potential window is limited by H^+ and Cl^-, as discussed above. Finally, Figure 3 clearly shows that the forward wave current depends on the presence of oxygen in solution. These observations lead us to conclude that the first current wave results from an assisted proton transfer reactions where the base is the oxygenated porphyrin Co–O_2(OEP), and that the second forward wave from the interfacial desorption to the organic phase of the protonated-oxygenated porphyrin, that is, Co–O_2H^+(OEP). The current of the reverse wave corresponds to the deprotonation of the oxygenated cobalt porphyrin being either adsorbed or present in the organic phase.

Recently, we reported a theoretical study on the cyclic voltammetry response for the transfer and desorption of charged surface–active molecules at liquid|liquid interfaces.[11] It has been shown that, as for cyclic voltammetry on a solid electrode, adsorption at the interface can cause the occurrence of pre- or post-peaks along with the usual voltammetric signal obtained for a reversible ion-transfer reaction controlled by semi-linear diffusion. In particular, we have shown that a clear distinction between adsorptive and diffusive phenomena is strongly dependent on the Gibbs energy of adsorption and that complex voltammetric signals could be obtained if the Gibbs energy of adsorption is moderate (< -20 kJ mol^{-1}). Here,

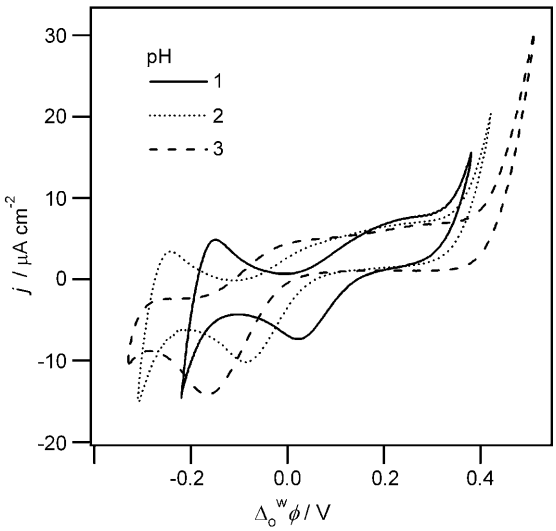

Figure 2. Cyclic voltammograms obtained (50 mV s^{-1}) at a water|1,2-DCE interface with cell 1 ($x = 200$) at different pH values, as indicated.

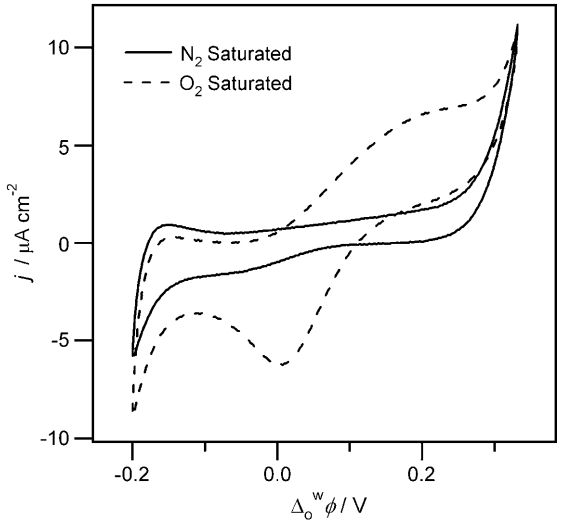

Figure 3. Cyclic voltammograms obtained at a water|1,2-DCE interface using cell 1 with $x = 200$ under N_2-saturated (——) and O_2-saturated (-----) conditions.

the first peak on the forward scan corresponds to an assisted proton-transfer reaction controlled by the diffusion of Co–O_2(OEP) in the organic phase, followed by a desorption peak of Co–O_2H^+(OEP). The close proximity between the two signals does not allow a clear differentiation and it is therefore difficult to estimate the Gibbs energy of adsorption of the adsorbed Co–O_2H^+(OEP) species.

Oxygen Reduction by Co(OEP)

Two-phase reactions were performed by mixing a 1,2-DCE solution containing 5 mM BATB and 200 μM Co(OEP) together with an aqueous solution containing 5 mM lithium tetrakis(pentafluorophenyl) borate diethyl etherate (LiTB) and 10 mM HCl in a small flask, as shown in Figure 4a. The Galvani potential difference across the water|1,2-DCE interface was polarized at a very positive value of 0.54 V calculated by the distribution of the two salts, LiTB and BATB with a common anion TB^-. At such potential values, protons can be transferred from water to 1,2-DCE and the aqueous TB^- ions act as a proton pump in the organic phase. As the supporting electrolyte concentration is in excess compared to that of Co(OEP), we can assume that the Galvani potential difference is not affected by the oxygen reduction reaction. After 30 min of stirring, the two phases were separated from each other and analyzed. When only Co(OEP) was present, the color and UV/Vis spectrum of the 1,2-DCE phase changed; red shifts of the original Soret (λ_{max} = 390 nm) and Q bands (λ_{max} = 515, 550 nm) were observed, which indicates that a reaction took place.[12] Indeed, the UV/Vis spectrum, which is ascribed to the oxygenation of Co(OEP) with formation of superoxide adduct, considered formally as [(Co^{III}-$O_2^{\cdot-}$)OEP] exhibits bands at λ_{max} = 409, 523, and 557 nm, as shown in Figure 4b when using only 5 μM of Co(OEP).

The isolated aqueous solution was titrated with NaI to detect the formation of H_2O_2. Thus, 0.1 M of NaI was added to 1 mL of the solution, and the color changed from colorless to

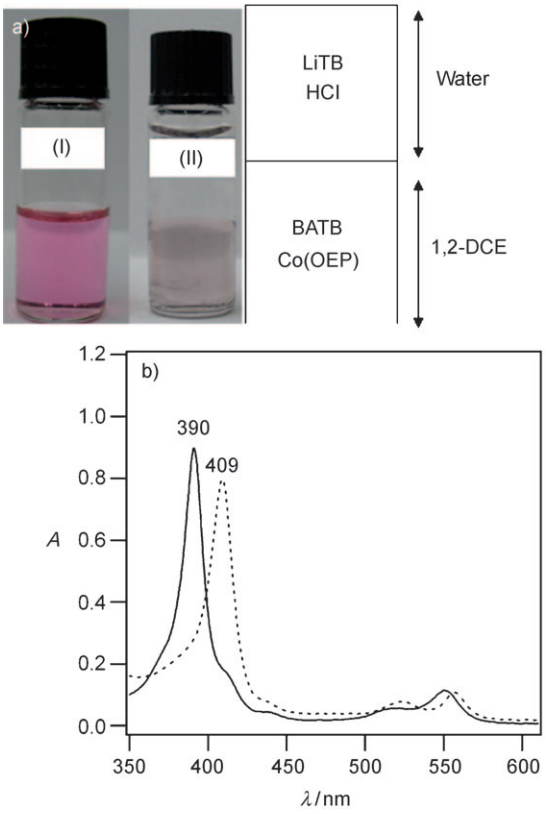

Figure 4. a) Two-phase reaction before (I) and after (II) 30 min shaking: the top aqueous phase containing 5 mM LiTB + 10 mM HCl; the bottom 1,2-DCE phase contained 5 mM BATB + 200 μM Co(OEP) in the flask. b) Absorption spectra of 5 μM Co(OEP) in 1,2-DCE freshly prepared (——) and after a shake flask experiment (•••••).

pale yellow. Adding NaI to an aqueous solution containing 5 mM LiTB and 10 mM HCl in a controlled titration did not lead to any color changes within the present experimental timescale, thus confirming the presence of H_2O_2 in the aqueous solution of the experiment in Figure 4a. The produced I_3^- species can be also detected by UV/Vis spectroscopy, as shown in Figure SI-2 of the Supporting Information (sharp absorption bands at λ_{max} = 287, 352 nm). Taking a ε_{max} value of $2.76 \times 10^4\ M^{-1}\,cm^{-1}$,[13] the concentration of I_3^- can be calculated to be 0.023 mM. A time profile for the formation of H_2O_2 in the presence of Co(OEP) in the case of TB^- at two pH values was observed (see Figure SI-3 of the Supporting Information), which shows that the production of H_2O_2 occurs more efficiently at pH 1 than at pH 2.

Co(OEP) Catalyzed Oxygen Reduction by Ferrocene

Figure 5 compares the CVs obtained under different experimental conditions. First, in the presence of only Fc in 1,2-DCE under aerobic conditions, a small voltammetric wave with a half-wave potential at 0 V was observed, which corresponds to the transfer of ferrocenium (Fc^+) produced by a slow oxidation of Fc in air of the stock solution.[8,9c] However, when both Fc and Co(OEP) or Co(OEP) alone were dissolved in 1,2-DCE, an irreversible positive current signal at the end of the potential

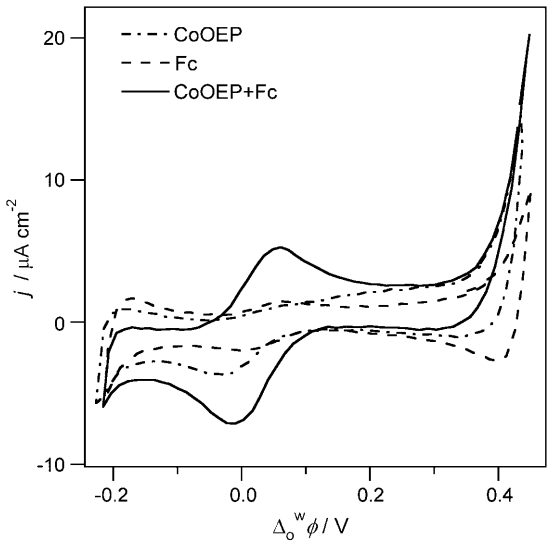

Figure 5. Cyclic voltammograms obtained at a water | 1,2-DCE interface with cell 2: $x=50$ and $y=0$ (–•–•), $x=0$ and $y=5$ (-----) and $x=50$ and $y=5$ (——).

range attributed to a PCET reaction can be observed. A control experiment under anaerobic conditions showed that this current signal is not present (data not shown). As observed previously with cobalt porphine[8] in the presence of Fc, this PCET reaction yields Fc^+, thus accounting for the significant increment of the Fc^+ transfer current wave located at 0 V, as shown in Figure 5. In fact, repeatedly cycling the potential to positive values, more Fc^+ will be produced, leading to a continuous increase of the Fc^+ transfer current. A control cyclic voltammetry measurement also proved that in the available potential window no reaction takes place between Fc in 1,2-DCE and H_2O_2 in acidic aqueous phase (see Figure SI-4 of the Supporting Information).

The reduction of O_2 by Fc was also studied by shake flask experiments performed as reported above.[8] The Galvani potential difference across the water | 1,2-DCE interface was polarized at a very positive value by using two salts, LiTB and BATB. As shown in Figure 6, 10 mM HCl was present in water in two flasks, and the 1,2-DCE phase contained only 5 mM Fc in flask a, 50 μM Co(OEP) and 5 mM Fc in flask b. It was observed

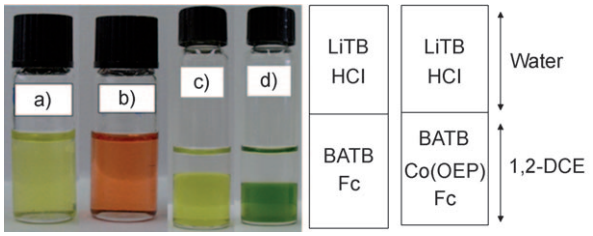

Figure 6. Photographs of two-phase reactions. The composition of the top aqueous phase is the same for the two flasks: 5 mM LiTB + 10 mM HCl, and the 1,2-DCE phase contains: a) a fresh solution of 5 mM Fc + 5 mM BATB; b) a fresh solution of 5 mM Fc + 50 μM Co(OEP) + 5 mM BATB; c) 5 mM Fc + 5 mM BATB after contacting with the water solution; d) 5 mM Fc + 50 μM Co(OEP) + 5 mM BATB after contacting with the water solution.

that the 1,2-DCE phase in flask b changed its color from orange to dark green immediately (flask d) after being put in contact with the water solution. In contrast, the 1,2-DCE phase in flask a remained the same (c). The two phases were then separated from each other for further spectroscopic and colorimetric tests.

First, UV/Vis spectra of the separated 1,2-DCE solutions were measured, as shown in Figure SI-5a of the Supporting Information. The formation of Fc^+ in the 1,2-DCE solution from flask d was revealed and the absorption band with a maximum at 620 nm represents its signature. The color change is thus due to the oxidation of Fc to Fc^+ and the color of the 1,2-DCE phase in flask d reflects a mixed color of green Fc^+ and orange Co(OEP). In contrast, in the presence of Fc, only in 1,2-DCE (flask c) no Fc^+ was detected, because no change in color and in the absorption spectrum (dotted black compared to full black) was observed. As for the isolated aqueous solutions from three flasks, an excess of NaI (equivalent to 0.1 M) was added. It was observed that the one from flask d changed from colorless to yellow (as illustrated in Figure SI-5b of the Supporting Information). As shown above, this color change can be due to the presence of H_2O_2 in the solution. In contrast, no H_2O_2 was detected at all in the aqueous solutions from flask c. The above-presented experimental facts clearly demonstrate that H_2O_2 and Fc^+ were produced in water and 1,2-DCE, respectively, only when both Fc and Co(OEP) were present (flask b). The concentration of I_3^- can be calculated to be 0.058 mM.

A time profile of the formation of Fc^+ in the absence and presence of Co(OEP) shows that the oxidation of Fc only takes place in the presence of Co(OEP). Upon addition of Co(OEP), the rise of the absorption bands at 620 nm, corresponding to Fc^+, could be immediately observed, as displayed in Figure 7a. In this experiment, the amount of ferrocenium produced, and of organic protons consumed, alters the distribution potential during the reaction. Figure 7b presents the calculated Galvani potential difference as a function of time based on the following assumptions:

i) To produce one mole of Fc^+ ions, one mole of protons has to be consumed.

ii) The system is always at thermodynamic equilibrium; therefore, the composition of the two phases will be dictated according to the Nernst equation and the concentration of ferrocenium as a function of time is read from Figure 7a.

iii) The electroneutrality condition is always fulfilled and the volume ratio between the two phases remains equal to unity.

Figure 7b clearly shows how the Galvani potential difference is modified during the course of the reaction as protons are being consumed and Fc^+ is produced. Briefly, after approximately 2 min there is a clear change in the slope of the Fc^+ appearance profile in Figure 7a. According to the calculations, the Galvani potential difference at 2 min corresponds to 0.49 V, which turns out to be 60 mV more negative than the standard ion-transfer potential of H^+. In consequence, the reaction rate will be appreciably diminished since the driving force for the proton-transfer reaction is lowered as the reaction proceeds.

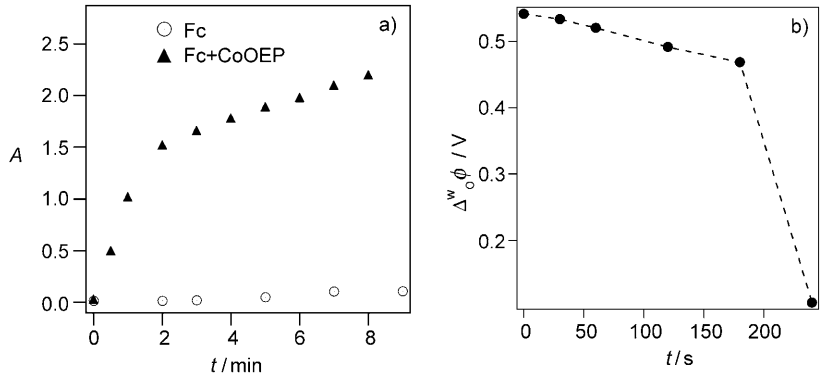

Figure 7. a) Time profile of the formation of Fc^+ in the absence (○) and presence (▲) of 50 μM Co(OEP) in 1,2-DCE during the shake flask experiments with TB^- as a common ion. b) Calculated Galvani potential difference using the ferrocenium concentration from Figure 7 a.

Mechanism

To interpret the data presented above, the following mechanism can be considered based on our recent work on amphiphilic cobalt porphyrins.[14] The first step is the oxygen binding step on Co(OEP). This complexation reaction can take place in the organic phase, and by tautomery we can obtain a Co^{III} complex [Eq. (1)]:

$$Co^{II}(OEP)_{(DCE)} + O_2 \rightarrow [Co^{II} - O_2(OEP)]_{(DCE)} \Leftrightarrow \left[Co^{III(+)} - O_2^{\cdot(-)}(OEP)\right]_{(DCE)} \quad (1)$$

When applying a positive potential, this complex can be protonated at the interface when in contact with aqueous protons. Some of the protonated complexes are likely to be adsorbed as shown by the voltammetric data of Figure 1 a, as described by Equation (2):

$$\left[Co^{III(+)} - O_2^{\cdot(-)}(OEP)\right]_{(DCE)} + H^+_{(w)} \rightarrow \left[Co^{III(+)} - O_2H^{\cdot}(OEP)\right]_{(ads/DCE)} \quad (2)$$

In the absence of ferrocene, the production of H_2O_2 observed in biphasic reactions shows that this complex is further reduced by Co(OEP) [Eq. (3)]. However, in the presence of ferrocene, the latter acts as the electron donor as observed by the production of ferrocenium in biphasic reactions [Eq. (4)]. Finally, in both cases the hyperoxide anion can then be protonated to form H_2O_2:

$$\left[Co^{III(+)} - O_2H^{\cdot}(OEP)\right]_{(ads/DCE)} + Co^{II}(OEP)_{(DCE)} \rightarrow [Co^{III}(OEP)]^+_{(DCE)} + O_2H^- \quad (3)$$

$$\left[Co^{III(+)} - O_2H^{\cdot}(OEP)\right]_{(ads/DCE)} + Fc_{DCE)} \rightarrow [Co^{III}OEP)]^+_{(DCE)} + Fc^+_{(DCE)} + O_2H^- \quad (4)$$

To compare the rate of oxygen reduction with and without ferrocene in the organic phase, we show in Figure 8 the rate of production of ferrocenium taken from Figure 7 and the rate of production of H_2O_2 taken from Figure SI-3 of the Supporting Information, both at pH 2. Although we do not compare exactly the same reaction product, we see that the normalized production of reaction products is somewhat faster in the presence of ferrocene. Indeed, as shown in Figure SI-6 of the Supporting Information—and as reported in Table 1—the standard redox potential for Co(OEP) is about 50 mV more positive than that of ferrocene (0.69 V vs 0.64 V) and ferrocene is a slightly better reducing agent.

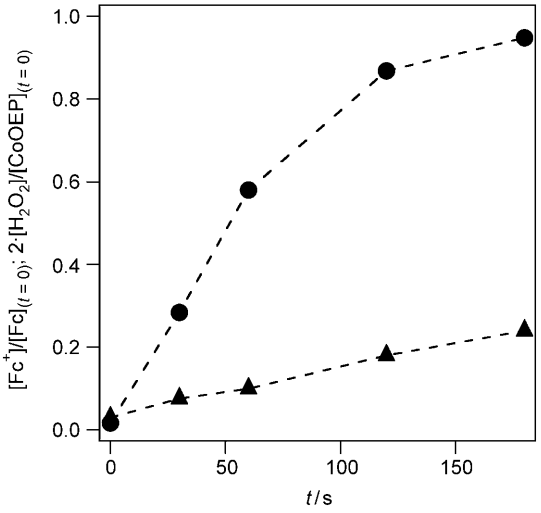

Figure 8. Comparison at pH 2 of the production of ferrocenium obtained with a concentration of 50 μM Co(OEP) + 5 mM Fc (●) and that of hydrogen peroxide in the presence of 200 μM Co(OEP) (▲) but normalized by the initial concentration of the electron donor.

Table 1. Data referred to 50 μM of porphyrin with 5 mM BATB supporting electrolyte in dry 1,2-DCE at 20 $mV\,s^{-1}$.[a]

Porphyrin	E_1 [V][b]	E_2 [V][b]	E_3 [V][b]
Co(OEP)	0.69	1.23	1.83

[a] Data extracted from Figure SI-5 of the Supporting Information. [b] Values measured versus the standard hydrogen electrode (SHE).

Conclusions

This study shows that Co(OEP) acts not only as a catalyst for the reduction of oxygen in the presence of electron donors such as ferrocene, but can also reduce O_2 directly. This reaction is another example of molecular electrocatalysis at soft interfaces. It has also been shown that adsorptive processes at the liquid | liquid interface play an important role in the catalytic effect observed for this porphyrin, thus allowing it to act as an ionophore for protons. All this evidence opens the way to the

study of catalytic self-assembled self-repairable monolayers at liquid|liquid interfaces.

Experimental Section

Chemical Reagents: All solvents and chemicals were used as received without further purification. LiTB was purchased from Aldrich. Hydrochloric acid (HCl), 1,2-dichloroethane (1,2-DCE, ≥99.8%), sodium iodide (NaI, >99.5%), tetramethylammonium chloride (TMACl, >98.0%), and bis(triphenylphosphoranylidene) ammonium chloride (BACl, ≥98%) were obtained from Fluka. Bis-(triphenylphosphoranylidene) ammoniumtetrakis(pentafluorophenyl)borate (BATB) was prepared by metathesis of 1:1 mixtures of BACl and LiTB in a methanol/water mixture (V:V = 2:1), followed by recrystallization from acetone. All the aqueous solutions were prepared with ultrapure water (18.2 MΩ cm^{-1}). The pH of the acidic aqueous solutions was adjusted by addition of HCl. Co(OEP) was synthesized following the typical procedure[10] and its molecular structure is illustrated in Scheme 2.

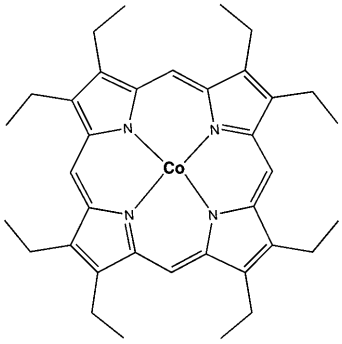

Scheme 2. Molecular structure of Co(OEP).

Voltammetry Measurements: Voltammetry measurements were carried out at the water|1,2-DCE interface in a four-electrode configuration using a conventional glass cell with a cross-section of 1.53 cm^2. Two silver|silver chloride (Ag|AgCl) wires positioned in two Luggin capillaries function as the reference electrodes to polarize the interface and two counter electrodes to provide the current. The electrolyte composition of the cells is illustrated in Scheme 1. The electrochemical experiments were performed on a commercial potentiostat (PGSTAT 30, EcoChemie, The Netherlands). The potential reported is the Galvani potential difference ($\Delta_0^w\phi$) obtained by correcting the applied potential with respect to the formal ion-transfer potential of tetramethylammonium (TMA^+) 0.16 V. The CVs during the second scan are presented, unless otherwise specified.

Two-Phase Reactions Controlled by the Distribution of the Supporting Electrolytes: Two-phase reactions were carried out in the presence of supporting electrolytes whose role is to control the Galvani potential difference between the two immiscible phases. These reactions were run in small flasks under magnetic stirring unless specially specified. A 1,2-DCE solution (2 mL) containing either 200 μM Co(OEP) or 5 mM Fc or 5 mM Fc + 50 μM Co(OEP) was added first, followed by the addition of 2 mL of an aqueous solution containing 10 mM HCl on the top. The supporting electrolytes, LiTB and BATB, were present at a concentration of 5 mM in the aqueous and 1,2-DCE phase, respectively. After stirring and further waiting for the clear separation of two phases, the aqueous and organic solutions were isolated from each other. The organic phase was directly subjected to UV/Vis spectroscopic measurements; the formed hydrogen peroxide (H_2O_2) in aqueous phase was checked by titration by iodide ion. Excess NaI (equivalent to 0.1 M) was added to 1 mL of aqueous solution after two-phase reaction in a round glass flask, and the formation of I_3^- was examined both by addition of Starch and by UV/Visi spectroscopy. The UV/Vis spectra were measured on an Ocean Optical CHEM2000 spectrophotometer with a quartz cuvette (path length = 10 mm).

Acknowledgements

This work was supported by EPFL, the Swiss National Science Foundation (FNRS 200020–116588), Centre National de la Recherche Scientifique (CNRS, UMR 5260), European COST Action (D36/007/06) and Grant Agency of the Czech Republic (no. 203/07/1257)

Keywords: cobalt · electrocatalysis · liquid|liquid interfaces · oxygen reduction · porphyrins

[1] M. W. Kanan, D. G. Nocera, *Science* **2008**, *321*, 1072–1075.
[2] a) E. E. Chufán, S. C. Puiu, K. D. Karlin, *Acc. Chem. Res.* **2007**, *40*, 563–572; b) J. P. Collman, R. A. Decreau, H. W. Lin, A. Hosseini, Y. Yang, A. Dey, T. A. Eberspacher, *Proc. Natl. Acad. Sci. USA* **2009**, *106*, 7320–7323.
[3] a) J. Rosenthal, D. G. Nocera, *Acc. Chem. Res.* **2007**, *40*, 543–553; b) J. P. Collman, R. Boulatov, C. J. Sunderland, L. Fu, *Chem. Rev.* **2004**, *104*, 561–588.
[4] K. M. Kadish, L. Fremond, Z. P. Ou, J. G. Shao, C. N. Shi, F. C. Anson, F. Burdet, C. P. Gros, J. M. Barbe, R. Guilard, *J. Am. Chem. Soc.* **2005**, *127*, 5625–5631.
[5] a) F. C. Anson, C. Shi, B. Steiger, *Acc. Chem. Res.* **1997**, *30*, 437; b) C. J. Chang, Y. Deng, C. Shi, C. K. Chang, F. C. Anson, D. G. Nocera, *Chem. Commun.* **2000**, *1355*; c) C. J. Chang, Z. H. Loh, C. Shi, F. C. Anson, D. G. Nocera, *J. Am. Chem. Soc.* **2004**, *126*, 10013.
[6] a) S. Fukuzumi, S. Mochizuki, T. Tanaka, *Inorg. Chem.* **1989**, *28*, 2459–2465; b) S. Fukuzumi, K. Okamoto, C. P. Gros, R. Guilard, *J. Am. Chem. Soc.* **2004**, *126*, 10441–10449.
[7] a) T. E. Bitterwolf, A. C. Ling, *J. Organomet. Chem.* **1972**, *40*, C29-C32; b) R. Prins, A. G. T. G. Kortbeek, *J. Organomet. Chem.* **1971**, *33*, C33; c) V. M. Fomin, *Russ. J. Gen. Chem.* **2007**, *77*, 954–960; d) V. M. Fomin, A. E. Shirokov, N. G. Polyakova, P. A. Smirnov, *Russ. J. Gen. Chem.* **2007**, *77*, 652–653.
[8] I. Hatay, B. Su, F. Li, M. Mendez, T. Khoury, C. P. Gros, J. M. Barbe, M. Ersoz, Z. Samec, H. H. Girault, *J. Am. Chem. Soc.* **2009**, *131*, 13453–13459.
[9] a) M. W. Urban, K. Nakamoto, J. Kincaid, *Inorg. Chim. Acta* **1982**, *61*, 77–81; b) R. D. Jones, D. A. Summerville, F. Basolo, *Chem. Rev.* **1979**, *79*, 139–179; c) R. Partovi-Nia, B. Su, F. Li, C. P. Gros, J. M. Barbe, Z. Samec, H. H. Girault, *Chem—Eur. J.* **2009**, *15*, 2335–2340.
[10] K. M. Kadish, K. M. Smith, Guilard, *In The Porphyrin Handbook Vol. 3*, Academic Press, New-York, **2000**.
[11] M. A. Méndez, B. Su, H. H. Girault, *J. Electroanal. Chem.* **2009**, *634*, 82–89.
[12] a) A. Salehi, W. A. Oertling, G. T. Babcock, C. K. Chang, *J. Am. Chem. Soc.* **1986**, *108*, 5630–5631; b) Z. Gasyna, M. J. Stillman, *Inorg. Chem.* **1990**, *29*, 5101–5109; c) C. Shi, F. C. Anson, *Inorg. Chem.* **2001**, *40*, 5829–5833; d) E. Schmidt, H. Zhang, C. K. Chang, G. T. Babcock, W. A. Oertling, *J. Am. Chem. Soc.* **1996**, *118*, 2954–2961.
[13] R. O. Rahn, M. I. Stefan, J. R. Bolton, E. Goren, P. S. Shaw, K. R. Lykke, *Photochem. Photobiol.* **2003**, *78*, 146–152.
[14] B. Su, I. Hatay, A. Trojanek, Z. Samec, T. Khoury, C. P. Gros, J.-M. Barbe, A. Daina, P.-A. Carrupt, H. H. Girault, *J. Am. Chem. Soc.* **2010**, *132*, 2655–2662.

Received: March 9, 2010
Published online on July 6, 2010

